Stem Cell Reports
Article

OPEN ACCESS

High-Level Precise Knockin of iPSCs by Simultaneous Reprogramming and Genome Editing of Human Peripheral Blood Mononuclear Cells

Wei Wen,[1] Xinxin Cheng,[1] Yawen Fu,[1] Feiying Meng,[1] Jian-Ping Zhang,[1] Lu Zhang,[1] Xiao-Lan Li,[1] Zhixue Yang,[1] Jing Xu,[1] Feng Zhang,[1] Gary D. Botimer,[6] Weiping Yuan,[1] Changkai Sun,[7,8,9,10] Tao Cheng,[1,2,3,4,5,*] and Xiao-Bing Zhang[1,11,*]

[1]State Key Laboratory of Experimental Hematology, Tianjin, China
[2]Institute of Hematology and Blood Disease Hospital, Chinese Academy of Medical Sciences and Peking Union Medical College, Tianjin, China
[3]Center for Stem Cell Medicine, Chinese Academy of Medical Sciences, Tianjin, China
[4]Department of Stem Cell & Regenerative Medicine, Peking Union Medical College, Tianjin, China
[5]Collaborative Innovation Center for Cancer Medicine, Tianjin, China
[6]Department of Orthopaedic Surgery, Loma Linda University, Loma Linda, CA, USA
[7]School of Biomedical Engineering, Faculty of Electronic Information and Electrical Engineering, Dalian University of Technology, Dalian 116024, China
[8]Research Center for the Control Engineering of Translational Precision Medicine, Dalian University of Technology, Dalian 116024, China
[9]State Key Laboratory of Fine Chemicals, Dalian R&D Center for Stem Cell and Tissue Engineering, Dalian University of Technology, Dalian 116024, China
[10]Liaoning Provincial Key Laboratory of Cerebral Diseases, Institute for Brain Disorders, Dalian Medical University, Dalian 116044, China
[11]Department of Medicine, Loma Linda University, Loma Linda, CA, USA
*Correspondence: chengtao@ihcams.ac.cn (T.C.), xzhang@llu.edu (X.-B.Z.)
https://doi.org/10.1016/j.stemcr.2018.04.013

SUMMARY

We have developed an improved episomal vector system for efficient generation of integration-free induced pluripotent stem cells (iPSCs) from peripheral blood mononuclear cells. More recently, we reported that the use of an optimized CRISPR-Cas9 system together with a double-cut donor increases homology-directed repair-mediated precise gene knockin efficiency by 5- to 10-fold. Here, we report the integration of blood cell reprogramming and genome editing in a single step. We found that expression of Cas9 and KLF4 using a single vector significantly increases genome editing efficiency, and addition of SV40LT further enhances knockin efficiency. After these optimizations, genome editing efficiency of up to 40% in the bulk iPSC population can be achieved without any selection. Most of the edited cells show characteristics of iPSCs and genome integrity. Our improved approach, which integrates reprogramming and genome editing, should expedite both basic research and clinical applications of precision and regenerative medicine.

INTRODUCTION

Induced pluripotent stem cells (iPSCs) have been recognized as an attractive cell source for stem cell therapy, drug discovery, and disease modeling (Takahashi et al., 2007; Takahashi and Yamanaka, 2006; Yu et al., 2007). Since blood cells can be easily obtained through a minimally invasive process and have been widely applied in clinical diagnosis, we and other investigators have been working on reprogramming of peripheral blood (PB) mononuclear cells (MNCs) in recent years (Agu et al., 2015; Chou et al., 2011, 2015; Diecke et al., 2015; Dowey et al., 2012; Hu et al., 2011; Liu et al., 2014; Loh et al., 2009; Mack et al., 2011; Meng et al., 2012; Merling et al., 2013; Su et al., 2013, 2016; Wen et al., 2016, 2017). More recently, we reported an efficient system for PB MNC reprogramming using an optimized combination of episomal vectors that express five reprogramming factors, and found that thousands of integration-free iPSC colonies can be generated from 1×10^6 PB MNCs (Wen et al., 2016, 2017). This seemingly simple but highly efficient system has been adopted by many other laboratories (Chou et al., 2015; Hu et al., 2015). The episomal vectors we used are plasmids carrying EBNA1 and oriP, which maintain the transgene expression for 1–2 weeks, allowing for successful reprogramming, and are gradually depleted from the cells during passage leading to generation of integration-free iPSCs.

For clinical regenerative medicine applications, patient-specific iPSCs, which often carry a disease-causing gene(s), have to be genome edited before differentiation into functional cells for therapy. CRISPR-Cas9 is a powerful genome editing technology to achieve this goal (Li et al., 2015; Park et al., 2015; Xie et al., 2014). CRISPR-Cas9 is an adoptive immune system evolved in bacteria and Archaea to fight against invading agents such as bacteriophages or plasmids (Wright et al., 2016), and has been successfully engineered to target the human genome (Hou et al., 2013). Diverse CRISPR systems have been adapted for use in editing iPSCs (Hou et al., 2013; Ran et al., 2015; Zetsche et al., 2015), among which the most commonly used system is derived from *Streptococcus pyogenes*. In this system, single guide RNA (sgRNA) guides endonuclease Cas9 to cleave a double-stranded DNA sequence of ~20 bp in length at 3 bp upstream of the protospacer adjacent motif (PAM) NGG. After double-stranded DNA cleavage, the damage is often repaired by error-prone non-homologous end joining (NHEJ) or precise homologous recombination

(HR) pathway (Hockemeyer et al., 2011; Yang et al., 2013). If a donor template that harbors both left and right homology arms is provided, the cells can be tricked to use the donor template to repair the damage instead of searching for the sister chromatids. As a result, a DNA fragment of interest can be precisely knocked in. However, this homology-directed repair (HDR)-mediated knockin system is far less efficient than gene knockout. In attempt to break this bottleneck in precise genome editing, we and other investigators developed a novel double-cut HDR donor, which is flanked by sgRNA recognition sequence and is released after CRISPR-Cas9 cleavage (Irion et al., 2014; Zhang et al., 2017). After optimization, we observed an ~5-fold increase in HDR efficiency using the double-cut donor with homology arms of 300–600 bp in length relative to circular plasmid donors (Zhang et al., 2017). Shortly after publication of our discovery, a similar study also reported the unprecedented editing efficiency of homology-mediated end joining compared with HR and microhomology-mediated end joining (Yao et al., 2017).

The conventional strategy of regenerative medicine is generation of iPSCs first followed by genome editing. However, this is a time-consuming and labor-intensive procedure that requires ~3 months of cell culture and two clone selections (Ding et al., 2013; Hockemeyer et al., 2009, 2011; Howden et al., 2011; Soldner et al., 2011; Yusa et al., 2011; Zou et al., 2009). To cut back on the time spent, one-step simultaneous reprogramming and CRISPR-Cas9 genome editing to generate gene-modified iPSCs from somatic cells has been proposed (Howden et al., 2015; Tidball et al., 2017). Howden et al. (2015) have reported generation of gene edited iPSCs from fibroblasts by nucleofection of episomal vectors expressing reprogramming factors and CRISPR-Cas9 vectors. They targeted a GFP reporter to the *DNMT3A* locus during reprogramming. They observed up to 5% GFP-positive edited cells in bulk cells, which is five times higher than that achieved by direct editing of iPSCs. These data provide the first evidence for the benefit of combining somatic cell reprogramming and genome editing in a single step. However, the use of fibroblasts from human skin biopsy is problematic because of the high mutation rate of skin cells after long-term exposure to UV light radiation and the invasive procedure used to procure the cells (Abyzov et al., 2012). In contrast to fibroblasts, PB cells are a preferable cell source for reprogramming (Zhang, 2013). As such, we attempted to generate gene edited iPSCs from PB MNCs by simultaneously reprogramming and gene editing.

In this study, we designed double-cut donors for HDR knockin of fluorescent reporters (Zhang et al., 2017). The knockin efficiency can be precisely determined by fluorescence-activated cell sorting (FACS) analysis of fluorescence-positive cells. A simple combination of reprogramming vectors and genome editing plasmids led to a nearly 10% knockin efficiency. Further improvements, including combining Cas9 and KLF4 expression in one vector and addition of SV40LT, increased HDR efficiency to up to 40%. Thus, in this study, we have established an optimized reprogramming and CRISPR-Cas9 system to efficiently generate gene-modified integration-free iPSCs directly from PB.

RESULTS

Simultaneous Reprogramming and Gene Editing to Generate Genome Edited iPSCs from PB MNCs

To generate gene-modified iPSCs, we transfected episomal vectors that express Yamanaka factors (OCT4, SOX2, MYC, and KLF4), and BCL-XL into PB MNCs after being cultured in erythroid medium for 6 days (Su et al., 2013, 2016; Wen et al., 2016). We additionally used a Cas9 episomal vector (Figure 1A), an sgRNA expressing plasmid vector that targets the end of *PRDM14* ORF sequence, and a double-cut donor plasmid as previously described (Zhang et al., 2017). The double-cut donor we designed was a promoterless GFP HDR donor that is flanked with sgPRDM14 recognition sequences (Figure 1B). After precise genome editing, the endogenous PRDM14 transcriptional machinery will drive the expression of both PRDM14 and GFP, which are linked with a self-cleaving E2A sequence (de Felipe et al., 2006). The length of both left and right homology arms is 600 bp, which is sufficient for high-level precise gene knockin (Zhang et al., 2017). After nucleofection, cells were cultured in optimized reprogramming conditions (Wen et al., 2017). Two weeks later, multiple iPSC-like colonies were observed. After four passages in culture, we analyzed the percentage of GFP-positive cells by flow cytometry (Figure 1C), which indicates the precise knockin efficiency at the *PRDM14* locus (Zhang et al., 2017). As a control, reprogramming factors (OS+B+M+K) only were used, which showed robust iPSC generation, but no knockin events were detected. After transfection of PB MNCs with both reprogramming factors and gene editing vectors (OS+B+M+K+Cas9+pD+sg), a 7%–8% knockin efficiency was observed in reprogrammed iPSCs (Figure 1D). In controls omitting Cas9 or sgPRDM14, no GFP-positive cells were detected (not shown), suggesting that the percentage of GFP-positive cells in experimental groups reflects HDR knockin efficiency.

To prevent artifacts associated with a certain genomic locus, we further assessed our system in two additional gene loci: *AAVS1* and *CTNNB1*. *AAVS1* locus was suggested as a safe harbor site that could be potentially targeted in gene therapy (Lombardo et al., 2011). *CTNNB1* encodes beta-catenin, a key protein in canonical WNT

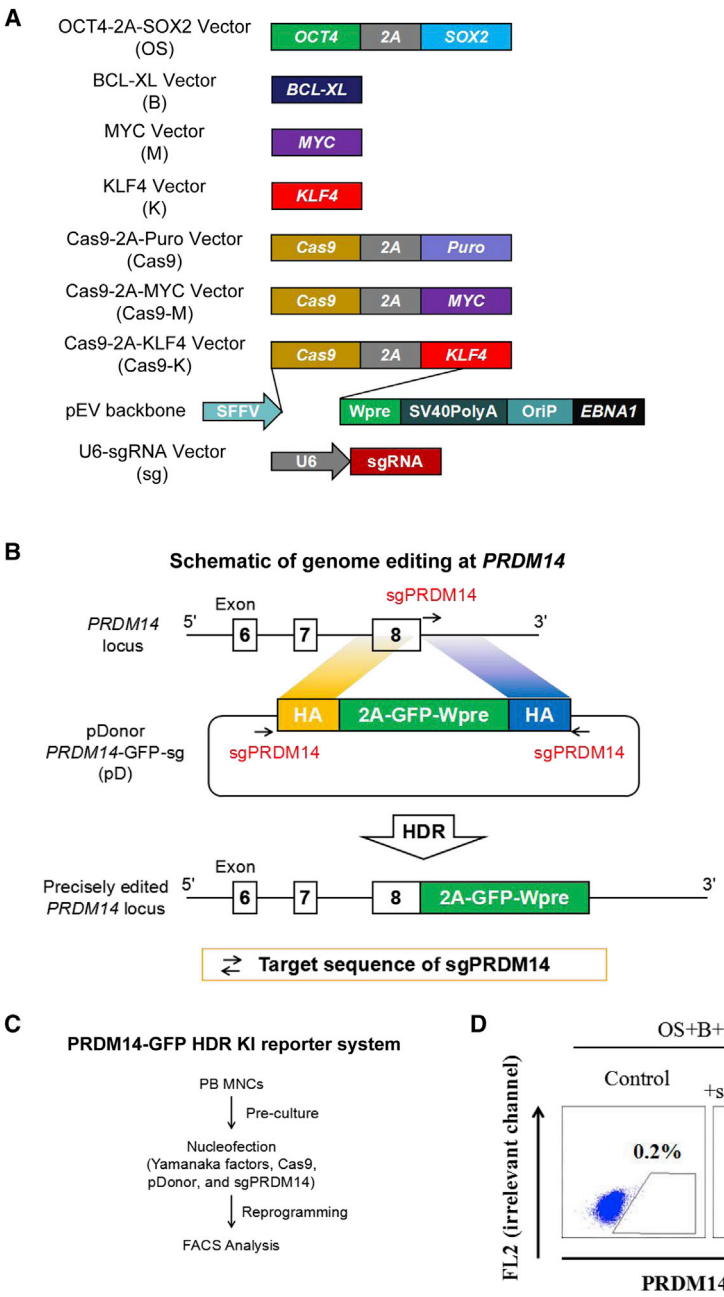

Figure 1. Efficient Generation of Gene-Modified iPSCs by Simultaneous Reprogramming and CRIPSR Genome Editing

(A) Schematic diagram of the episomal vector plasmids. SFFV is the spleen focus-forming virus U3 promoter. 2A (E2A) is a self-cleaving peptide derived from equine rhinitis A virus. Wpre, post-transcriptional regulatory element; SV40PolyA, polyadenylation signal from SV40 virus; OriP, EBV (Epstein-Barr virus) origin of replication; EBNA1, Epstein-Barr nuclear antigen 1.

(B) Schematic of genome editing at the *PRDM14* locus. An sgPRDM14 was designed to create a double-strand break (DSB) at 4 bp after the stop codon TAG as previously described. The double-cut donor (pD) contains a left homology arm (HA), a 2A-GFP-Wpre-polyA cassette, and a right HA. This double-cut donor is flanked with the sgPRDM14 target sequence.

(C) Schematic illustration of the overall experimental design.

(D) Representative FACS diagrams of iPSCs at passage 4 (P4) after PB MNC reprogramming by nucleofection with indicated episomal vectors. OS, pEV-SFFV-OCT4-2A-SOX2; B, pEV-SFFV-BCL-XL; M, pEV-SFFV-MYC; K, pEV-SFFV-KLF4. See also Figure S1.

pathway that is expressed in iPSCs (Kim et al., 2013; Lu et al., 2004). We designed sgRNAs targeting *AAVS1* or *CTNNB1* loci as well as the related two double-cut donors with 600 bp homology arms (Figures S1A, S1B, S1D, and S1E). Similarly, we transfected PB MNCs and assessed knockin efficiency after four passages. FACS analysis showed a knockin efficiency of 8%–10% in these two sites (Figures S1C and S1F). In controls without genome editing vectors, no GFP signal was detectable. In AAVS1 knockin donor vector, the EF1 promoter was used, which can drive the expression of GFP without integration. As such, we included controls that omit Cas9 or sgAAVS1. As expected, GFP was detectable shortly after transfection, but after reprogramming and four passages of culture, less than 0.01% cells were GFP$^+$ (not shown), suggesting that almost all the GFP$^+$ events in the experimental groups are due to precise insertion at the expected sites.

Taken together, we have achieved knockin efficiencies of up to 10% in three different loci after simultaneous reprogramming and gene editing. This efficiency is higher than a previous report (5%) (Howden et al., 2015).

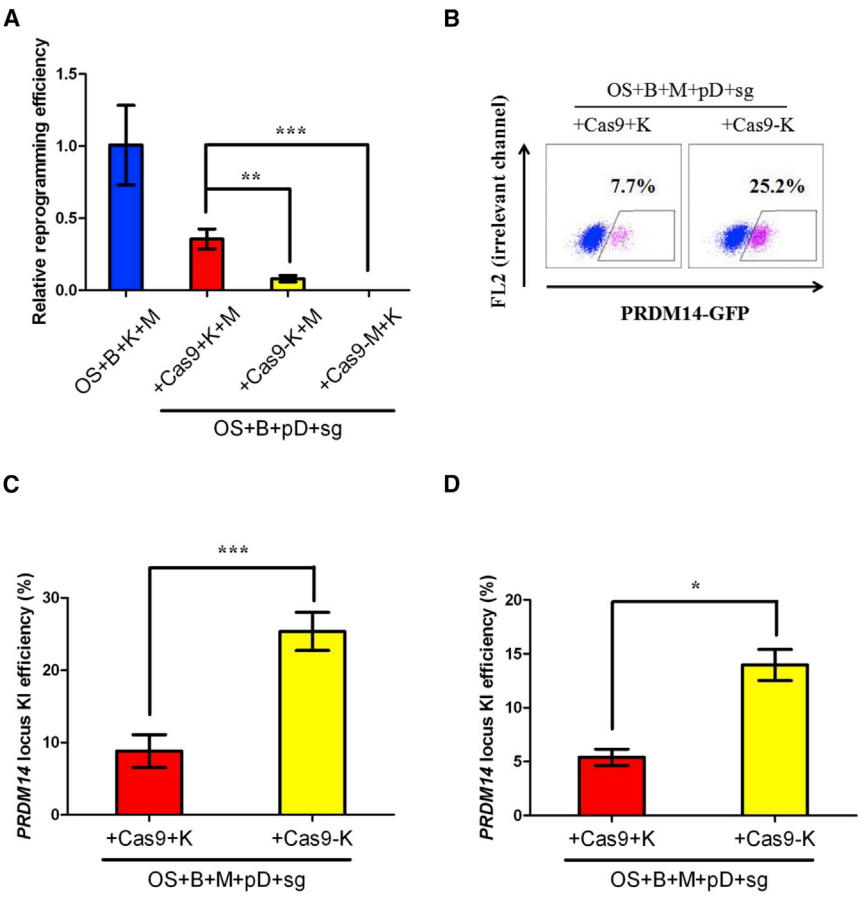

Figure 2. Increased Knockin Efficiency during PB MNC Reprogramming by Vector Optimization

(A) Relative PB MNC reprogramming efficiency using indicated episomal vectors. Since the seeding cell number in each group may be different, the colony numbers from each group were calculated from seeding 1×10^6 PB MNCs and normalized to the "OS+B+M+K" control group. Data shown are mean ± SEM from three independent experiments. $^{**}p < 0.01$; $^{***}p < 0.001$.

(B) Representative FACS diagrams of iPSCs at passage 4 (P4) after PB MNC reprogramming by nucleofection with indicated episomal vectors. Percentage of GFP^+ cells represents knockin efficiency.

(C and D) Knockin efficiency at *PRDM14* of iPSCs at P4 from two different blood donors. Data shown are mean ± SEM from three independent experiments. $^{*}p < 0.05$; $^{***}p < 0.001$. See also Figure S2.

Increasing Knockin Efficiency of Reprogrammed iPSCs by Vector Optimization

Previously, we have reported that the use of one vector to express OCT4 and SOX2 (linked by a 2A self-cleaving peptide), and expressing MYC and KLF individually, can lead to high-efficiency reprogramming of PB MNCs, whereas other combinations considerably decrease the efficiency (Wen et al., 2016). This finding indicates that a small change in vector design can have a big impact. In order to increase the knockin efficiency during reprogramming, we compared several vector combinations. We used one vector expressing both Cas9 and one Yamanaka factor by a 2A linker to replace two vectors expressing Cas9 and the reprogramming factor individually (Figure 1A). Since expression of OCT4 and SOX2 in one vector is critical to successful reprogramming, we constructed two episomal vectors: pEV-SFFV-Cas9-E2A-MYC (Cas9-2A-M or Cas9-M) and pEV-SFFV-Cas9-E2A-KLF4 (Cas9-2A-K or Cas9-K). When PB MNCs were nucleofected with Cas9-2A-M, together with other reprogramming and editing factors, we observed no iPSC-like colony formation even at 18 days after transfection. In comparison, a decent number of colonies could be obtained in combinations including Cas9-2A-K (Figure 2A). Interestingly, knockin efficiency at *PRDM14* locus was 2- to 3-fold higher in the Cas9-2A-K group compared with the Cas9+K group ($p < 0.05$) (Figures 2B and 2C). We further tested PB MNCs from a different donor, and observed the same level of increase in knockin efficiency with Cas9-2A-K versus Cas9+K (Figure 2D).

Besides the *PRDM14* locus, we also tested the *AAVS1* and *CTNNB1* loci. Again, we observed ~2-fold higher levels of knockin in the Cas9-2A-K group than the control Cas9+K group (Figures S2). Collectively, our data demonstrate that using a single episomal vector to express Cas9 endonuclease and reprogramming factor KLF4 significantly increases gene editing efficiency of reprogrammed iPSCs.

SV40LT Further Increases Knockin Efficiency in Our Optimized Cas9-2A-K System

We have shown enhanced knockin efficiency with the Cas9-2A-K system compared with the Cas9+K individual expression system. However, the reprogramming efficiency dramatically decreased in the Cas9-2A-K system. To rescue the defect of the new vector system in reprogramming, we screened a series of pluripotency factors in attempts to identify factors that can increase reprogramming efficiency

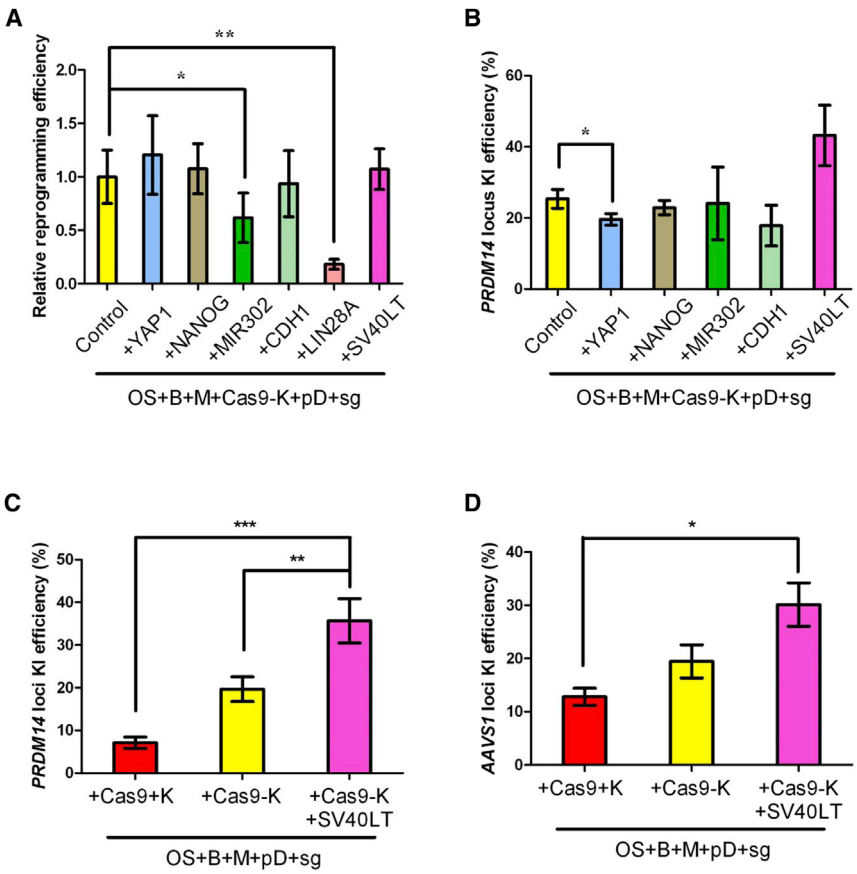

Figure 3. SV40LT Increases Knockin Efficiency in Our Optimized System

(A) Relative PB MNC reprogramming efficiency using indicated episomal vectors. The colony numbers from each group are normalized to the control group. Data shown are mean ± SEM from three independent experiments. *p < 0.05; **p < 0.01.

(B) Knockin efficiency at *PRDM14* of iPSCs at P4 after reprogramming. Data shown are mean ± SEM from three independent experiments. *p < 0.05.

(C) SV40LT increases knockin efficiency at the *PRDM14* locus. Data shown are mean ± SEM from six independent experiments using three different blood cells donors. **p < 0.01; ***p < 0.001.

(D) SV40LT increases knockin efficiency at the *AAVS1* locus. Data shown are mean ± SEM from four independent experiments using three different blood cells donors. *p < 0.05.

See also Figure S3.

but do not decrease knockin efficiency. We evaluated several factors with demonstrated positive effects on somatic cell reprogramming. Overexpression of the transcriptional regulator YAP1, one of the downstream effectors of the Hippo pathway (Qin et al., 2012), has been reported to increase the efficiency of mouse iPSC generation (Lian et al., 2010). NANOG is a well-known booster of somatic cell reprogramming (Yu et al., 2007). LIN28A plays a positive role in reprogramming of fibroblasts from both humans and mice (Yu et al., 2007). SV40LT considerably enhances blood cell reprogramming (Chou et al., 2011). CDH1, also known as E-Cadherin, is critical for mouse embryonic stem cell pluripotency and can enhance reprogramming of mouse fibroblasts (Chen et al., 2010; Redmer et al., 2011). In addition, MIR302, a microRNA that is highly expressed in embryonic stem cells and has been reported to greatly promote reprogramming (Miyoshi et al., 2011). We cloned the aforementioned factors into our episomal vector carrying a strong SFFV promoter, and added them back individually in the Cas9-2A-K system, followed by assessing their effects on both reprogramming and gene editing. Reprogramming efficiency was determined by counting the number of alkaline phosphatase (AP)-positive colonies. AP is considered a universal pluripotency marker for all types of pluripotent stem cells, including iPSCs. We found that addition of YAP1, NANOG, or CDH1 did not show obvious changes in PB reprogramming efficiency in the Cas9-2A-K system, and MIR302 even slightly decreased reprogramming efficiency. Most surprisingly, and in contrast to previous reports on the positive effects of LIN28A in fibroblast reprogramming (Yu et al., 2007), we found that LIN28A strongly inhibited PB MNC reprogramming in the Cas9-2A-K reprogramming and editing system (Figures 3A and S3A). To further consolidate this conclusion, we added LIN28A in the PB reprogramming system without genome editing vectors (OS+B+M+K). Still, LIN28A decreased PB reprogramming by almost 100-fold (OS+B+M+K versus OS+B+M+K+LIN28A) (Figure S3B). As for SV40LT, we observed increased reprogramming, but no statistical significance was achieved in some experiments (Figures 3A, S3D, and S3E).

Genome editing efficiency at the *PRDM14* locus was determined by flow cytometry after HDR knockin of the GFP reporter. We observed no obvious changes in editing efficiency when NANOG, YAP1, CDH1, or MIR302 was added in the control Cas9-2A-K group. However, inclusion of SV40LT almost doubled the knockin efficiency at the *PRDM14* locus (Figures 3B, 3C, and S3C). To validate this

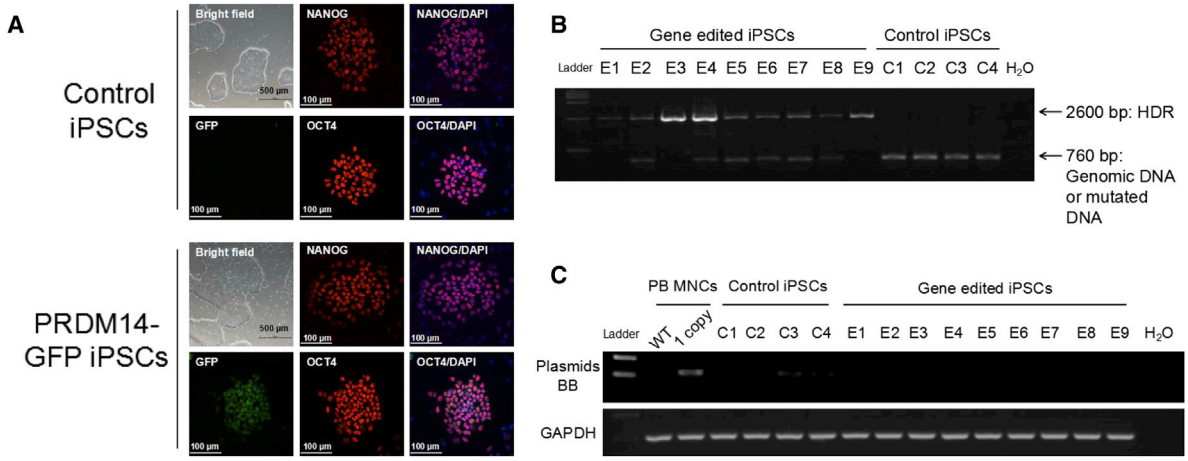

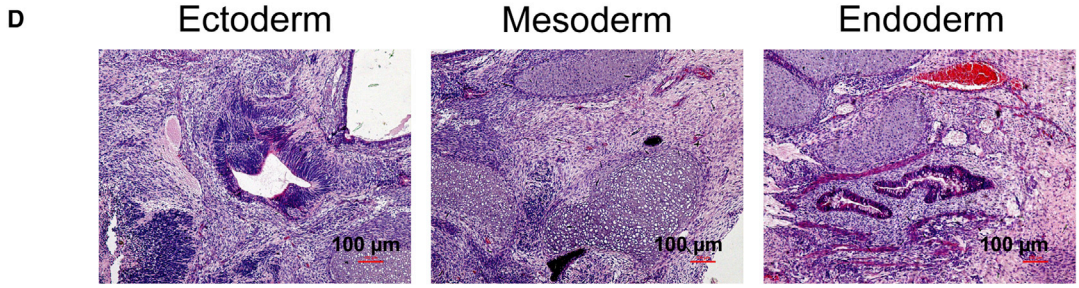

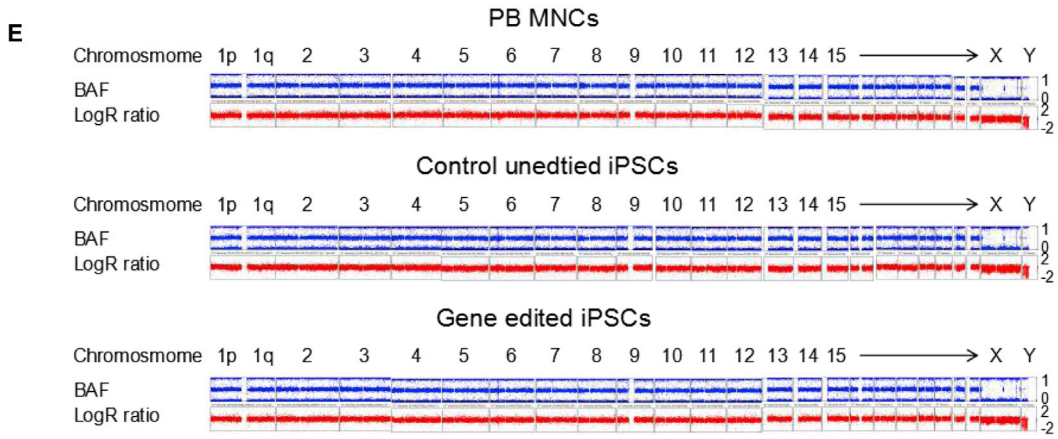

F

Summary of digital karyotyping

	PB MNCs	Control iPSCs	Gene edited iPSCs
Normal	2	9	10
Abnormal	0	0	1
Total	2	9	11

(legend on next page)

finding, we tested the effects of SV40LT in editing another site, *AAVS1*. Again, we observed a 50% increase (~20% knockin for without SV40LT versus ~30% for with SV40LT) (Figure 3D).

Taken together, the optimized editing while reprogramming system with the use of both Cas9-2A-K and SV40LT led to an up to 4-fold increase in HDR genome editing efficiency (Figures 3C and 3D).

Characterization of Genome Edited iPSCs Generated with Optimized System from PB MNCs

To determine whether genome editing during blood cell reprogramming affects the quality of iPSCs, we conducted single-cell cloning by FACS sorting GFP-positive cells at passage 2 after editing and reprogramming. iPSC colonies generated from the same blood samples but without CRISPR vectors were used as controls. After five passages, over 98% of *PRDM14* gene edited iPSCs were GFP positive (data not show). These cells showed typical morphology of human iPSCs and expressed pluripotency markers like NANOG and OCT4 (Figures 4A and S4A).

We next assessed whether knockin at the *PRDM14* locus is through HDR. PCR amplification of the target sequence of nine randomly selected PRDM14-GFP$^+$ clones showed a predicted 2.6 kb band after HDR editing, which was absent in control unedited iPSCs (Figure 4B). Among these clones, 33% showed a single 2.6 kb band, indicating biallelic editing. Sequencing of the 2.6 kb bands showed that the cells were precisely edited by HDR (Figure S4B). In all the heterozygous clones, we observed indel mutations on the allele without knockin (Figure S4C).

We further assessed the copy number of GFP in edited clones by qPCR. Seven out of nine clones show one or two copies (Figure S4D), which is consisted with monoallelic or biallelic HDR knockin of GFP (Figure 4B). However, we found increased GFP copy number of 2.5 for one monoallelic HDR editing and of 3 for biallelic editing, suggestive of one random insertion of GFP fragment in each clone.

Our previous data showed that episomal vector plasmids are rapidly depleted from cells and thus integration-free iPSCs can be established (Wen et al., 2016). Similarly, using specific primers targeting plasmid backbone, none or less than one copy of residual plasmids in gene edited iPSC colonies were detected after five passages (Figure 4C). These data suggest that transient expression of vectors for reprogramming and editing is sufficient for generation of integration-free gene edited iPSCs in a single step.

We then assessed genome integrity by digital karyotyping, which allows for identification of deletion or duplication of small piece of DNAs that would otherwise be invisible by conventional G-banding karyotyping analysis. To this purpose, nine iPSC colonies generated by episomal reprogramming without gene editing (OS+B+M+K) and 11 iPSC colonies generated by simultaneously reprogramming and gene editing (OS+B+M+Cas9-2A-K+pD+sg+SV40LT) were analyzed using Human Core Exome arrays (D'Antonio et al., 2017). All these iPSC colonies were derived from two donors. We did not detect any copy number variants (CNVs) in two PB MNC control samples and nine reprogrammed but not edited iPSC clones (Figures 4E, S5, and S6). In addition, 10 out of 11 reprogrammed and edited iPSC clones also showed normal karyotyping, while we identified an alteration on chromosome 5 in one gene edited iPSC clone (clone E8; Figure S5). Although these results invoke caution, there was no statistical difference in karyotypic abnormalities between edited and unedited iPSCs (Fisher's exact test; p = 0.55.) (Figure 4F).

We also examined the pluripotency by teratoma assay. Representative clones of edited and unedited iPSCs (three edited clones and two unedited clones) were injected into NOD/SCID immunodeficient mice. Two to 3 months later, teratomas were dissected for histological analysis. Both types of iPSCs were differentiated into cells representative of three germ layers, indicating that genome editing does not affect the iPSC pluripotency (Figure 4D).

Collectively, we conclude that integration-free iPSCs generated by simultaneous reprogramming and gene editing are indistinguishable from reprogrammed but unedited cells in morphology, phenotype, karyotype, and pluripotency.

Figure 4. Characterization of Genome Edited iPSCs Generated with Optimized System

(A) Morphology and confocal images of representative iPSC clones.

(B) Determination of monoallelic versus biallelic HDR editing at *PRDM14*. Nine edited clones were analyzed.

(C) PCR analysis of residual plasmids in iPSCs. Specific primers for plasmid backbone (BB) were used to amplify all the vectors. GAPDH serves as a DNA loading control. One copy of residual plasmid was mimicked by mixing of 1.6 pg of Cas9-2A-K plasmid with 1 μg of genomic DNA. Unedited iPSCs were generated with OS+B+M+K. Gene edited iPSCs were generated with "OS+B+M+Cas9-2A-K+pD-PRDM14+sgPRDM14+SV40LT".

(D) H&E staining shows teratomas representative of three germ layers from gene edited iPSCs.

(E) Digital karyotyping arrays of donor PB MNCs and generated iPSC lines. Unedited iPSCs were generated with OS+B+M+K. Gene edited iPSCs were generated with OS+B+M+Cas9-2A-K+pD-PRDM14+sgPRDM14+SV40LT. BAF, B allele frequency.

(F) A summary of digital karyotyping as in (E). For Fisher's exact test, the p value was calculated by formula $p = (a + b)!\,(c + d)!\,(a + c)!\,(b + d)!/[a!b!c!d!\,(a + b + c + d)!] = 0.55$, in which a = 9, b = 10, c = 0, and d = 1. See also Figure S4.

Table 1. Detailed Information of Indels Induced at On-Target Sites

	Indel (bp)	Reads (%)
Donor 1 with No SV40LT (total reads = 52,124)		
TGAAGACTACTAGCCCT|GCCAGG	0	34.73
TGAAGACTACTAGCCCTtGCCAGG	+1	42.21
TGAAGACTACTAGC————CAGG	−5	7.17
TGAAGACTACTAGCCCTctGCCAG	+2	1.52
TGAAGACTACTAGC-CTGCCAGG	−1	1.49
TGAAGACTACTAGCCCTcctGCC	+3	0.83
TGAAGACTACTA————————	−24	0.55
TGAA————————————————————	−25	0.54
TGAAGACTACTAGCCCcTGCCAGG	+1	0.51
Donor 1 with pEV-SV40LT (total reads = 27,253)		
TGAAGACTACTAGCCCT|GCCAGG	0	18.78
TGAAGACTACTAGCCCTtGCCAGG	+1	45.84
TGAAGACTACTA————GCCAGG	−5	8.79
TGAAGACTACTAGCC-TGCCAGG	−1	1.83
TGAAGACTACTAGCCCTctGCCAG	+2	1.40
TGAAGACTACTAGC–TGCCAGG	−2	1.16
TGAAGACTACTA——————————G	−10	0.94
TGAAGACTACTAGCCCTcctGCCA	+3	0.81
TGAAGACTACTAGC——CCAGG	−4	0.78
TGAAGACTACTAGCCC-GCCAGG	−1	0.70
TGAAGACTACTA—————————GG	−9	0.65
TGAAGACTACT—————GCCAGG	−6	0.64
TGAAGACTACTAGCC————————	−10	0.56
TGAAGACTACTAGCC————————	−24	0.52
Donor 1 with pSFFV-SV40LT (total reads = 96,422)		
TGAAGACTACTAGCCCT|GCCAGG	0	15.80
TGAAGACTACTAGCCCTtGCCAGG	+1	48.50
TGAAGACTACTAGCC————AGG	−5	11.64
TGAAGACTACTAGCCTGCC-AGG	−1	1.88
TGAAGACTACTAGCCCTctGCCAG	+2	1.60
TGAAGACTACTAG———————————	−10	1.10
TGAAGACTACTAGCCC-GCCAGG	−1	1.05
TGAAGACTACTAGC–TGCCAGG	−2	1.04
TGAAGACTACTAGCCCTcctGCCA	+3	0.96
TGAAGACTACTAG———————G	−9	0.93
TGAAGACT————————————————	−25	0.86
TGAAGACTACTAGCCC——AGG	−4	0.60
TGAAGACTACTAG————————	−24	0.59
TGAAGACTAC—————TGCCAGG	−6	0.58
TGAAGACTA—————TGCCAGG	−7	0.54
TGA—————————————————————	−28	0.54
TGAAGACTACTAGCCCT—————	−8	0.50

The underlining indicates insert mutations. See also Table S1.

Analysis of On-Target Cleavage and Off-Target Effects by High-Throughput Sequencing

Finally, we evaluated on-target cleavage and off-target effects in reprogrammed and edited cells. We analyzed iPSCs generated (1) without SV40LT; (2) with episomal pEV-SV40LT; and (3) with pSFFV-SV40LT, a regular SV40LT expressing plasmid vector. We compared pEV with regular plasmid to determine whether regular plasmid leads to rapid depletion of SV40LT vector. To our surprise, we found no significant difference in dynamics of vector depletion between pEV-SV40LT and pSFFV-SV40LT by qPCR (Figure S4E). We then analyzed PCR products of on-target and off-target sites by Illumina sequencing. We observed high levels of indel mutations (from 65% to 91%) in all edited iPSCs (Tables 1 and 2, and S1). Of interest, we found the inclusion of SV40LT tended to increase on-target cleavage relative to control (81% for pEV versus 88% for plasmid versus 67% for no SV40LT) (Tables 1 and S1). In four out of six edited iPSC samples, absolutely no off-target effects were detected. Of interest, in two samples treated with pEV-SV40LT, we detected low levels (0.15% and 0.08%) of indel cleavage in 1 out 15 putative off-target sites (PRDM14-off12). Taken together, we detected high-level on-target and very-low-level off-target cleavage in our system.

DISCUSSION

Building upon our blood cell episomal reprogramming system and an efficient double-cut donor-mediated knockin strategy, here we have reported a simultaneous PB cell reprogramming and CRISPR-Cas9 gene editing method. Although this is not the first report on establishing gene edited iPSCs directly from somatic cells, our

Table 2. Frequencies of Indels Induced at On-Target and Off-Target Sites

Amplicon Name	sgRNA Sequence	Donor 1 No SV40LT	Donor 1 pEV-SV40LT	Donor 1 pSFFV-SV40LT	Donor 2 No SV40LT	Donor 2 pEV-SV40LT	Donor 2 pSFFV-SV40LT
PRDM14-On	GAAGACTACTAGCCCTGCCAGG	65.27% (52124)	81.22% (27253)	84.2% (96422)	69.76% (29570)	81.6% (67887)	90.94% (54961)
PRDM14-Off1	AATGACTAgCTAGCCCTGCCCGG	ND (274018)	ND (62373)	ND (212254)	ND (59100)	ND (51196)	ND (97940)
PRDM14-Off2	GAGGCCTAC-AGCCCTGCCTGG	ND (623372)	ND (219831)	ND (681736)	ND (144926)	ND (272086)	ND (326654)
PRDM14-Off3	CATGACTAC-AGCCCTGCCTGG	ND (517147)	ND (153567)	ND (499286)	ND (114781)	ND (135985)	ND (226137)
PRDM14-Off4	GA-GCCTAGTAGCCCTGCCAGG	ND (237917)	ND (55138)	ND (190509)	ND (53336)	ND (57903)	ND (79913)
PRDM14-Off5	CCAGACT-CTAGCCCTGCCTGG	ND (249580)	ND (73936)	ND (212231)	ND (55696)	ND (39869)	ND (64505)
PRDM14-Off6	CA-GACTACAAGCCCTGCCAGG	ND (421130)	ND (114951)	ND (576702)	ND (237009)	ND (352201)	ND (592115)
PRDM14-Off7	-AAGCCTACGAGCCCTGCCTGG	ND (118176)	ND (32067)	ND (86715)	ND (21460)	ND (19937)	ND (39503)
PRDM14-Off8	GATGACTA-TAGCCCTGCCTGG	ND (1182307)	ND (293821)	ND (1057123)	ND (331444)	ND (481926)	ND (826539)
PRDM14-Off9	GAAGGA-ACTAGCCCTGCCAGG	ND (462623)	ND (124231)	ND (425694)	ND (111054)	ND (141785)	ND (218065)
PRDM14-Off10	GAtAGAATAATAGCCCTGCCTGG	ND (201885)	ND (59918)	ND (172790)	ND (42014)	ND (33211)	ND (55286)
PRDM14-Off11	GAAGTTCTCCTAGCCCTGCCAGG	ND (7777)	ND (3705)	ND (9608)	ND (1880)	ND (1175)	ND (1651)
PRDM14-Off12	-AAGACCACAAGCCCTGCCTGG	ND (1168826)	0.15% (162553)	ND (1173091)	ND (307115)	0.08% (450589)	ND (741222)
PRDM14-Off13	GAACACAAC-AGCCCTGCCAGG	ND (998855)	ND (294816)	ND (838294)	ND (295574)	ND (414908)	ND (735881)
PRDM14-Off14	GAGGACTAC-AGCCCTGCCAGG	ND (52104)	ND (14858)	ND (60649)	ND (17841)	ND (13982)	ND (19550)
PRDM14-Off15	GATGCCTAC-AGCCCTGCCCGG	ND (339253)	ND (75118)	ND (345323)	ND (67702)	ND (38205)	ND (69752)

ND, not detected. The numbers indicate total reads.

optimized vector system is ~10 times more efficient than the previous report in generating gene edited iPSCs from somatic cells in one step (Howden et al., 2015).

The use of our optimized vector system can lead to high-level reprogramming and precise genome editing in a single step. Although the reprogramming efficiency is reduced with Cas9-2A-K compared with our previously optimized combination of episomal vectors (Wen et al., 2016, 2017), we can still routinely obtain ~100 iPSC colonies from 1 mL of PB when using OS+B+M+Cas9-2A-K+pD+sg+SV40LT. High-level gene editing efficiency of 20%–40% is attributable to two improvements: (1) the expression of Cas9 and KLF4 in a single vector, and (2) the inclusion of SV40LT. We observed that expression of KLF4 and Cas9 in one vector leads to a striking decrease of reprogramming efficiency and a significant increase in editing efficiency. This can be explained by the unique vector design. On the one hand, the compound vector decreased KLF4 expression in transfected cells, thereby leading to low-level reprogramming. On the other hand, all the successfully reprogrammed cells expressed relatively high levels of Cas9, which has contributed to improved DNA cleavage and HDR editing. We anticipate that the combination of Cas9 and KLF4 in one vector may also improve genome editing efficiency in systems other than blood cell reprogramming.

Of interest, the combination of MYC and Cas9 in one vector failed to generate any iPSC clones, which is reminiscent of our previous report that expression of MYC and KLF4 driven by one promoter leads to a 100-fold decrease in reprogramming compared with expression of the two factors individually (Wen et al., 2016). These data suggest that high-level MYC is critical for successful blood cell reprogramming. In support of this argument, recent reports have demonstrated that MYC controls human pluripotent stem cell fate decisions and pluripotency surveillance (Cliff et al., 2017; Díaz-Díaz et al., 2017).

To further increase reprogramming efficiency, we screened multiple factors that were reported to have positive effects on reprogramming in certain cell types. We show that YAP1, NANOG, MIR302, and CDH1 have no obvious positive effects on blood cell reprogramming. In contrast to the reported positive effect of LIN28A on fibroblast reprogramming, we found that it strikingly suppresses PB MNC reprogramming. It is likely that our highly efficient vector combination has saturated the blood cell reprogramming system; thereby it masked unpronounced effects of many other factors identified in less efficient systems.

Interestingly, SV40LT increases gene knockin efficiency in our optimized Cas9-2A-K system. The mechanism of SV40LT-mediated increase in HDR knockin is unclear and deserves further investigation. Our data show an increase of on-target cleavage efficiency from 60%–70% to ~90% after addition of SV40LT, which may have led to an increase in knockin efficiency.

Although SV40LT has shown roles in tumorigenesis and chromosome instability (Ahuja et al., 2005; Boichuk et al., 2010), we observed only one clone (1/11) that showed an alteration on chromosome 5, and no statistically significant differences in genome integrity between unedited versus edited iPSCs have been achieved. We speculate that transient expression of SV40LT during reprogramming may not be sufficient for transformation and inducing chromosome instability, but it still calls for caution.

A recent paper reported an up to 50% gene knockout efficiency while reprogramming (Tidball et al., 2017). Since NHEJ-mediated knockout is much more efficient than HDR-mediated knockin, efficient knockout and reprogramming in a single step can be also achieved using our approach by simply omitting the donor template. In support of this argument, we observed up to 90% indel mutations in the bulk population of *PRDM14* edited iPSCs. In our study we used a double-cut donor plasmid to guide HDR editing; we believe that our optimized system using Cas9-2A-K and SV40LT should also increase editing efficiency when ssODN (single-strand oligo donor) donors are used (Yoshimi et al., 2016).

We also addressed the off-target effects in our reprogramming/editing system. We only observed low-level (0.08%–0.15%) cleavage in 1 out of 15 predicted off-target sites when pEV-SV40LT was used. However, iPSCs generated with regular SV40LT expressing plasmid did not show any off-target effects, while SV40LT expressed by both vectors increased editing efficiency to the same level. These data suggest that, in the future, SV40LT plasmid instead of pEV-SV40LT may be used in simultaneous reprogramming/editing systems to enhance editing efficiency while minimizing off-target cleavage.

Generation of integration-free iPSCs can also be achieved using Sendai virus (Fusaki et al., 2009) or RNA transfection (Warren et al., 2010). Similarly, Cas9 RNA or protein together with modified sgRNA can replace Cas9-sgRNA expressing plasmids for genome editing, even with higher DNA cleavage efficiency (Kim et al., 2014). However, our system, based on episomal vectors and plasmid vectors, is easy to use, widely applicable, and more affordable.

In summary, we have identified an optimized combination of episomal reprogramming vectors and CRISPR-Cas9 genome editing vectors to achieve simultaneous high-level HDR knockin and reprogramming of PB MNCs into iPSCs. The gene editing efficiency is up to 40%, which is 10 times higher than the previous report. This simple and affordable approach will not only increase research productivity but also minimize the accumulation of mutations by decreasing culture time from 3–4 months to 1–2 months.

EXPERIMENTAL PROCEDURES

Episomal Vectors

The majority of episomal vectors used in this study have been reported earlier (Su et al., 2013, 2016; Wen et al., 2016, 2017). Briefly, plasmids MYC (M), KLF4 (K), and BCL-XL (B) were constructed by inserting the open reading frames of MYC, KLF4, and BCL-XL into the episomal vector backbone, respectively. Plasmid OCT4-2A-SOX2 (OS), Cas9-2A-Puro (Cas9), Cas9-2A-MYC (Cas9-2A-M), and Cas9-2A-KLF4 (Cas9-2A-K) were constructed by inserting the open reading frames of OCT4-2A-SOX2, Cas9-2A-Puro, Cas9-2A-MYC, and Cas9-2A-KLF4 into the episomal vector backbone, respectively. The 2A peptide from equine rhinitis A virus was used to link two genes as previously described (Wen et al., 2016; Zhang et al., 2016).

sgRNA Design

sgRNAs were designed using the Web-based program CHOPCHOP (https://chopchop.rc.fas.harvard.edu/) (Montague et al., 2014) to target areas in close proximity to the stop codons of human *CTNNB1* and human *PRDM14* genes and on intron 1 of human *PPP1R12C* gene (for *AAVS1*) (Zhang et al., 2017). We preferentially chose sgRNAs with a G at the 5′ end which initiates U6-promoter-mediated transcription. Three sgRNAs were used in this study: sgCTNNB1 (GCTGATTGCTGTCACCTGG), sgPRDM14 (GAAGACTACTAGCCCTGCC), and sgAAVS1 (GGGGCCACTAGG GACAGGAT).

Donor Plasmid Construction

To construct donor plasmids targeting the *PRDM14* stop codon, the left and right homology arms were amplified from human genomic DNA, with the stop codon being removed and in-frame linked with the 2A sequence; the insert 2A-GFP-Wpre-polyA was amplified from another vector in the laboratory. A sgPRDM14 target sequence together with the PAM sequence (GGAAGACTAC TAGCCCTGCCAGG) was tagged to the regions flanking the upstream and downstream homology arm (HA) (Zhang et al., 2017).

PB MNCs

Human PB was obtained from Tianjin Blood Center with approval of the local research ethics committee (approval number: KT2017005-EC-1). MNCs were obtained by standard density gradient centrifugation with Ficoll-Hypaque (1.077 g/mL) (G&E Healthcare; 17-1440-03) at room temperature and were cultured in erythroid medium for 6 days before nucleofection as previously described (Su et al., 2013, 2016; Wen et al., 2016, 2017).

Genome Editing and Reprogramming

Vectors for genome editing and reprogramming were transferred to PB MNCs by nucleofection. Vectors were extracted using Endofree Plasmid Maxi Kit (Qiagen; 12362). We prepared indicated plasmids in a sterile Eppendorf tube, followed by heating the tube at 50°C for 5 min to prevent contamination. The dosage of each plasmid was: OS, 2 μg; B, 0.5 μg; M, 1 μg; K, 1 μg; Cas9, 3 μg; Cas9-2A-M, 4 μg; Cas9-2A-K, 4 μg; pD (PRDM14, CTNNB1, or AAVS1), 2 μg; sg (PRDM14, CTNNB1, or AAVS1), 1 μg; YAP1, 1 μg; NANOG, 1 μg; MIR302, 1 μg; LIN28A, 1 μg; SV40LT, 1 μg; CDH1, 1 μg. After cool-down to room temperature, 57 μL of nucleofection buffer and 13 μL of supplement were added (Lonza; VPA-1003). PB MNCs were harvested by centrifugation at 200 × *g* for 7 min, 2×10^6 PB MNCs were nucleofected with indicated plasmids, and 1×10^5 to 2×10^6 cells were plated in each well of six-well plates with inactivated mouse embryonic fibroblast (MEF) feeder cells being seeded 1 day before nucleofection. We used the U-008 program following the manufacturer's protocol (Lonza; Nucleofector 2b). Culture medium was gradually switched to E8 medium as previously described (Su et al., 2013, 2016; Wen et al., 2016, 2017). From day 0–14, cells were cultured in hypoxia (3% O_2). After day 14–18 post nucleofection, the bulk populations of iPSCs were ready for passage and FACS analysis.

Single-Cell Cloning

iPSCs were dissociated using Accutase to prepare single-cell suspension, followed by single-cell sorting immediately into 96-well plates coated with Matrigel (BD; 354277). Single-cell sorting was conducted using a BD FACS Aria III with a 70 mm nozzle under sterile conditions. Each well contained 100 μL of E8 medium supplemented with ROCK inhibitor Y-27632 (10 μM). After sorting, cells were cultured at 37°C with 5% CO_2. Colony formation was seen 7 days after sorting. The cells were refreshed with E8 medium every 2 to 3 days (Zhang et al., 2017).

On-Target and Off-Target Cleavage Analysis

Two weeks after nucleofection, ~1,000 colonies from each group were harvested for analysis. We predicted top 15 putative off-target sites using a Web-based program (https://crispr.bme.gatech.edu/) and designed primers to amplify on-target sites and these putative off-target sites (Table S2). The PCR cycling conditions were: 95°C for 4 min followed by 98°C for 5 s, 64°–68°C for 10 s, 72°C for 10 s, for 30 cycles. High-throughput sequencing of PCR products was performed by Novogene using Hiseq-PE (paired end) 150. Data were analyzed using the Web-based program Galaxy (https://usegalaxy.org/). For clarity, we presented indels with reads of >0.5% of on-target cleavage.

Digital Karyotyping

Genomic DNA samples from indicated iPSCs were hybridized to HumanCoreExome arrays (Illumina, 20005132), and stained and scanned using the Illumina HiScan system per standard protocol (D'Antonio et al., 2017). Several algorithms have been used to detect CNVs, among which Log R ratio (LRR) and B allele frequency (BAF) are the commonly used methods. Because LRR is the logged ratio of observed probe intensity to expected intensity, any deviations from zero in this metric indicate copy number changes, while BAF is the proportion of hybridized sample that carries the B allele as designated by the Infinium assay. Thus, a normal sample would have discrete BAFs of 0.0, 0.5, and 1.0 for each locus (representing AA, AB, and BB).

Statistics

Data were analyzed by paired student's t test or Wilcoxon test whenever appropriate. *$p < 0.05$; **$p < 0.01$; ***$p < 0.001$; ns, not significant.

SUPPLEMENTAL INFORMATION

Supplemental Information includes Supplemental Experimental Procedures, six figures, and two tables can be found with this article online at https://doi.org/10.1016/j.stemcr.2018.04.013.

AUTHOR CONTRIBUTIONS

X.-B.Z. conceived of and supervised the study. W.W., X.C., Y.F., F.M., J.-P.Z., L.Z., X.-L.L., Z.Y., J.X., F.Z., and X.-B.Z. conducted the experiments. W.W., X.C., J.-P.Z., L.Z., J.X., F.Z., Y.F., F.M., and X.-B.Z. analyzed the results. W.W., G.D.B., W.Y., C.S., T.C., and X.-B.Z. wrote the paper. All authors reviewed the manuscript. All authors read and approved the final manuscript.

ACKNOWLEDGMENTS

This work was supported by grants from the Ministry of Science and Technology of China (2016YFA0100600, 2015CB964902, 2012CB966601), the National Natural Science Foundation of China (81770198, 81700184, 81700183, 81570164, 81500148, 81421002, 81730006), CAMS Initiative for Innovative Medicine (2016-I2M-1-017, 2017-I2M-2-001, 2017-I2M-B&R-04), CAMS Fundamental Research Funds for Central Research Institutes (2016GH3100001), the National Science and Technology Major Special Project on Major New Drug Innovation (2012ZX09503-001-003), Fundamental Research Funds for the Central Universities (DUT16ZD227, DUT17ZD222, DUT18ZD301), and the Loma Linda University School of Medicine GCAT grant (2015).

Received: December 11, 2017
Revised: April 13, 2018
Accepted: April 16, 2018
Published: May 10, 2018

REFERENCES

Abyzov, A., Mariani, J., Palejev, D., Zhang, Y., Haney, M.S., Tomasini, L., Ferrandino, A., Belmaker, L.A.R., Szekely, A., Wilson, M., et al. (2012). Somatic copy-number mosaicism in human skin revealed by induced pluripotent stem cells. Nature *492*, 438–442.

Agu, C.A., Soares, F.A.C., Alderton, A., Patel, M., Ansari, R., Patel, S., Forrest, S., Yang, F., Lineham, J., Vallier, L., et al. (2015). Successful generation of human induced pluripotent stem cell lines from blood samples held at room temperature for up to 48 hr. Stem Cell Reports *5*, 660–671.

Ahuja, D., Sáenz-Robles, M.T., and Pipas, J.M. (2005). SV40 large T antigen targets multiple cellular pathways to elicit cellular transformation. Oncogene *24*, 7729.

Boichuk, S., Hu, L., Hein, J., and Gjoerup, O.V. (2010). Multiple DNA damage signaling and repair pathways deregulated by Simian virus 40 large T antigen. J. Virol. *84*, 8007–8020.

Chen, T., Yuan, D., Wei, B., Jiang, J., Kang, J., Ling, K., Gu, Y., Li, J., Xiao, L., and Pei, G. (2010). E-Cadherin-mediated cell–cell contact is critical for induced pluripotent stem cell generation. Stem Cells *28*, 1315–1325.

Chou, B.-K., Gu, H., Gao, Y., Dowey, S.N., Wang, Y., Shi, J., Li, Y., Ye, Z., Cheng, T., and Cheng, L. (2015). A facile method to establish human induced pluripotent stem cells from adult blood cells under feeder-free and xeno-free culture conditions: a clinically compliant approach. Stem Cells Transl. Med. *4*, 320–332.

Chou, B.-K., Mali, P., Huang, X., Ye, Z., Dowey, S.N., Resar, L.M.S., Zou, C., Zhang, Y.A., Tong, J., and Cheng, L. (2011). Efficient human iPS cell derivation by a non-integrating plasmid from blood cells with unique epigenetic and gene expression signatures. Cell Res. *21*, 518–529.

Cliff, T.S., Wu, T., Boward, B.R., Yin, A., Yin, H., Glushka, J.N., Prestegaard, J.H., and Dalton, S. (2017). MYC controls human pluripotent stem cell fate decisions through regulation of metabolic flux. Cell Stem Cell *21*, 502–516.e9.

D'Antonio, M., Woodruff, G., Nathanson, J.L., D'Antonio-Chronowska, A., Arias, A., Matsui, H., Williams, R., Herrera, C., Reyna, S.M., Yeo, G.W., et al. (2017). High-throughput and cost-effective characterization of induced pluripotent stem cells. Stem Cell Reports *8*, 1101–1111.

Díaz-Díaz, C., Fernandez de Manuel, L., Jimenez-Carretero, D., Montoya, M.C., Clavería, C., and Torres, M. (2017). Pluripotency surveillance by Myc-driven competitive elimination of differentiating cells. Dev. Cell *42*, 585–599.e4.

de Felipe, P., Luke, G.A., Hughes, L.E., Gani, D., Halpin, C., and Ryan, M.D. (2006). E unum pluribus: multiple proteins from a self-processing polyprotein. Trends Biotechnol. *24*, 68–75.

Diecke, S., Lu, J., Lee, J., Termglinchan, V., Kooreman, N.G., Burridge, P.W., Ebert, A.D., Churko, J.M., Sharma, A., Kay, M.A., et al. (2015). Novel codon-optimized mini-intronic plasmid for efficient, inexpensive, and xeno-free induction of pluripotency. Sci. Rep. *5*, 8081.

Ding, Q., Lee, Y.-K., Schaefer, E.A.K., Peters, D.T., Veres, A., Kim, K., Kuperwasser, N., Motola, D.L., Meissner, T.B., Hendriks, W.T., et al. (2013). A TALEN genome editing system to generate human stem cell-based disease models. Cell Stem Cell *12*, 238–251.

Dowey, S.N., Huang, X., Chou, B.-K., Ye, Z., and Cheng, L. (2012). Generation of integration-free human induced pluripotent stem cells from postnatal blood mononuclear cells by plasmid vector expression. Nat. Protoc. *7*, 2013–2021.

Fusaki, N., Ban, H., Nishiyama, A., Saeki, K., and Hasegawa, M. (2009). Efficient induction of transgene-free human pluripotent stem cells using a vector based on Sendai virus, an RNA virus that does not integrate into the host genome. Proc. Jpn. Acad. Ser. B Phys. Biol. Sci. *85*, 348–362.

Hockemeyer, D., Soldner, F., Beard, C., Gao, Q., Mitalipova, M., DeKelver, R.C., Katibah, G.E., Amora, R., Boydston, E.A., Zeitler, B., et al. (2009). Highly efficient gene targeting of expressed and silent genes in human ESCs and iPSCs using zinc finger nucleases. Nat. Biotechnol. *27*, 851–857.

Hockemeyer, D., Wang, H., Kiani, S., Lai, C.S., Gao, Q., Cassady, J.P., Cost, G.J., Zhang, L., Santiago, Y., Miller, J.C., et al. (2011). Genetic engineering of human ES and iPS cells using TALE nucleases. Nat. Biotechnol. *29*, 731–734.

Hou, Z., Zhang, Y., Propson, N.E., Howden, S.E., Chu, L.-F., Sontheimer, E.J., and Thomson, J.A. (2013). Efficient genome engineering in human pluripotent stem cells using Cas9 from *Neisseria meningitidis*. Proc. Natl. Acad. Sci. USA *110*, 15644–15649.

Howden, S.E., Gore, A., Li, Z., Fung, H.-L., Nisler, B.S., Nie, J., Chen, G., McIntosh, B.E., Gulbranson, D.R., Diol, N.R., et al. (2011). Genetic correction and analysis of induced pluripotent stem cells from a patient with gyrate atrophy. Proc. Natl. Acad. Sci. USA *108*, 6537–6542.

Howden, S.E., Maufort, J.P., Duffin, B.M., Elefanty, A.G., Stanley, E.G., and Thomson, J.A. (2015). Simultaneous reprogramming and gene correction of patient fibroblasts. Stem Cell Reports *5*, 1109–1118.

Hu, J., Wang, Y., Jiao, J., Liu, Z., Zhao, C., Zhou, Z., Zhang, Z., Forde, K., Wang, L., Wang, J., et al. (2015). Patient-specific cardiovascular progenitor cells derived from integration-free induced pluripotent stem cells for vascular tissue regeneration. Biomaterials *73*, 51–59.

Hu, K., Yu, J., Suknuntha, K., Tian, S., Montgomery, K., Choi, K.-D., Stewart, R., Thomson, J.A., and Slukvin, I.I. (2011). Efficient generation of transgene-free induced pluripotent stem cells from normal and neoplastic bone marrow and cord blood mononuclear cells. Blood *117*, e109.

Irion, U., Krauss, J., and Nüsslein-Volhard, C. (2014). Precise and efficient genome editing in zebrafish using the CRISPR/Cas9 system. Development *141*, 4827–4830.

Kim, H., Wu, J., Ye, S., Tai, C.-I., Zhou, X., Yan, H., Li, P., Pera, M., and Ying, Q.-L. (2013). Modulation of β-catenin function maintains mouse epiblast stem cell and human embryonic stem cell self-renewal. Nat. Commun. *4*, 2403.

Kim, S., Kim, D., Cho, S.W., Kim, J., and Kim, J.-S. (2014). Highly efficient RNA-guided genome editing in human cells via delivery of purified Cas9 ribonucleoproteins. Genome Res. *24*, 1012–1019.

Li, H.L., Fujimoto, N., Sasakawa, N., Shirai, S., Ohkame, T., Sakuma, T., Tanaka, M., Amano, N., Watanabe, A., Sakurai, H., et al. (2015). Precise correction of the dystrophin gene in Duchenne muscular dystrophy patient induced pluripotent stem cells by TALEN and CRISPR-Cas9. Stem Cell Reports *4*, 143–154.

Lian, I., Kim, J., Okazawa, H., Zhao, J., Zhao, B., Yu, J., Chinnaiyan, A., Israel, M.A., Goldstein, L.S.B., Abujarour, R., et al. (2010). The role of YAP transcription coactivator in regulating stem cell self-renewal and differentiation. Genes Dev. *24*, 1106–1118.

Liu, S.P., Li, Y.X., Xu, J., Gu, H.H., Zhang, H.Y., Liang, H.Y., Liu, H.Z., Zhang, X.B., Cheng, T., and Yuan, W.P. (2014). An improved method for generating integration-free human induced pluripotent stem cells. Zhongguo Shi Yan Xue Ye Xue Za Zhi *22*, 580–587.

Loh, Y.-H., Agarwal, S., Park, I.-H., Urbach, A., Huo, H., Heffner, G.C., Kim, K., Miller, J.D., Ng, K., and Daley, G.Q. (2009). Generation of induced pluripotent stem cells from human blood. Blood *113*, 5476–5479.

Lombardo, A., Cesana, D., Genovese, P., Di Stefano, B., Provasi, E., Colombo, D.F., Neri, M., Magnani, Z., Cantore, A., Lo Riso, P., et al. (2011). Site-specific integration and tailoring of cassette design for sustainable gene transfer. Nat. Methods *8*, 861–869.

Lu, W., Yamamoto, V., Ortega, B., and Baltimore, D. (2004). Mammalian Ryk is a Wnt coreceptor required for stimulation of neurite outgrowth. Cell *119*, 97–108.

Mack, A.A., Kroboth, S., Rajesh, D., and Wang, W.B. (2011). Generation of induced pluripotent stem cells from CD34+ cells across blood drawn from multiple donors with non-integrating episomal vectors. PLoS One *6*, e27956.

Meng, X., Neises, A., Su, R.-J., Payne, K.J., Ritter, L., Gridley, D.S., Wang, J., Sheng, M., William Lau, K.H., Baylink, D.J., et al. (2012). Efficient reprogramming of human cord blood CD34+ cells into induced pluripotent stem cells with OCT4 and SOX2 alone. Mol. Ther. *20*, 408–416.

Merling, R.K., Sweeney, C.L., Choi, U., De Ravin, S.S., Myers, T.G., Otaizo-Carrasquero, F., Pan, J., Linton, G., Chen, L., Koontz, S., et al. (2013). Transgene-free iPSCs generated from small volume peripheral blood nonmobilized CD34^{+} cells. Blood *121*, e98.

Miyoshi, N., Ishii, H., Nagano, H., Haraguchi, N., Dewi, D.L., Kano, Y., Nishikawa, S., Tanemura, M., Mimori, K., Tanaka, F., et al. (2011). Reprogramming of mouse and human cells to pluripotency using mature microRNAs. Cell Stem Cell *8*, 633–638.

Montague, T.G., Cruz, J.M., Gagnon, J.A., Church, G.M., and Valen, E. (2014). CHOPCHOP: a CRISPR/Cas9 and TALEN web tool for genome editing. Nucleic Acids Res. *42*, W401–W407.

Park, C.-Y., Kim, D.H., Son, J.S., Sung, J.J., Lee, J., Bae, S., Kim, J.-H., Kim, D.-W., and Kim, J.-S. (2015). Functional correction of large factor VIII gene chromosomal inversions in hemophilia A patient-derived iPSCs using CRISPR-Cas9. Cell Stem Cell *17*, 213–220.

Qin, H., Blaschke, K., Wei, G., Ohi, Y., Blouin, L., Qi, Z., Yu, J., Yeh, R.-F., Hebrok, M., and Ramalho-Santos, M. (2012). Transcriptional analysis of pluripotency reveals the Hippo pathway as a barrier to reprogramming. Hum. Mol. Genet. *21*, 2054–2067.

Ran, F.A., Cong, L., Yan, W.X., Scott, D.A., Gootenberg, J.S., Kriz, A.J., Zetsche, B., Shalem, O., Wu, X., Makarova, K.S., et al. (2015). In vivo genome editing using *Staphylococcus aureus* Cas9. Nature *520*, 186–191.

Redmer, T., Diecke, S., Grigoryan, T., Quiroga-Negreira, A., Birchmeier, W., and Besser, D. (2011). E-cadherin is crucial for embryonic stem cell pluripotency and can replace OCT4 during somatic cell reprogramming. EMBO Rep. *12*, 720–726.

Soldner, F., Laganiere, J., Cheng, A.W., Hockemeyer, D., Gao, Q., Alagappan, R., Khurana, V., Golbe, L.I., Myers, R.H., Lindquist, S., et al. (2011). Generation of isogenic pluripotent stem cells differing exclusively at two early onset Parkinson point mutations. Cell *146*, 318–331.

Su, R.-J., Baylink, D.J., Neises, A., Kiroyan, J.B., Meng, X., Payne, K.J., Tschudy-Seney, B., Duan, Y., Appleby, N., Kearns-Jonker, M., et al. (2013). Efficient generation of integration-free iPS cells from human adult peripheral blood using BCL-XL together with Yamanaka factors. PLoS One *8*, e64496.

Su, R.J., Neises, A., and Zhang, X.-B. (2016). Generation of iPS cells from human peripheral blood mononuclear cells using episomal vectors. In Induced Pluripotent Stem (iPS) Cells: Methods and Protocols, K. Turksen and A. Nagy, eds. (Springer New York), pp. 57–69.

Takahashi, K., Tanabe, K., Ohnuki, M., Narita, M., Ichisaka, T., Tomoda, K., and Yamanaka, S. (2007). Induction of pluripotent stem cells from adult human fibroblasts by defined factors. Cell *131*, 861–872.

Takahashi, K., and Yamanaka, S. (2006). Induction of pluripotent stem cells from mouse embryonic and adult fibroblast cultures by defined factors. Cell *126*, 663–676.

Tidball, A.M., Dang, L.T., Glenn, T.W., Kilbane, E.G., Klarr, D.J., Margolis, J.L., Uhler, M.D., and Parent, J.M. (2017). Rapid generation of human genetic loss-of-function iPSC lines by simultaneous reprogramming and gene editing. Stem Cell Reports *9*, 725–731.

Warren, L., Manos, P.D., Ahfeldt, T., Loh, Y.-H., Li, H., Lau, F., Ebina, W., Mandal, P., Smith, Z.D., Meissner, A., et al. (2010). Highly efficient reprogramming to pluripotency and directed differentiation of human cells using synthetic modified mRNA. Cell Stem Cell *7*, 618–630.

Wen, W., Zhang, J.-P., Chen, W., Arakaki, C., Li, X., Baylink, D., Botimer, G.D., Xu, J., Yuan, W., Cheng, T., et al. (2017). Generation of integration-free induced pluripotent stem cells from human peripheral blood mononuclear cells using episomal vectors. J. Vis. Exp. https://doi.org/10.3791/55091.

Wen, W., Zhang, J.-P., Xu, J., Su, R.J., Neises, A., Ji, G.-Z., Yuan, W., Cheng, T., and Zhang, X.-B. (2016). Enhanced generation of integration-free iPSCs from human adult peripheral blood mononuclear cells with an optimal combination of episomal vectors. Stem Cell Reports *6*, 873–884.

Wright, A.V., Nuñez, J.K., and Doudna, J.A. (2016). Biology and applications of CRISPR systems: harnessing nature's toolbox for genome engineering. Cell *164*, 29–44.

Xie, F., Ye, L., Chang, J.C., Beyer, A.I., Wang, J., Muench, M.O., and Kan, Y.W. (2014). Seamless gene correction of β-thalassemia mutations in patient-specific iPSCs using CRISPR/Cas9 and piggyBac. Genome Res. *24*, 1526–1533.

Yang, H., Wang, H., Shivalila, C.S., Cheng, A.W., Shi, L., and Jaenisch, R. (2013). One-step generation of mice carrying reporter and conditional alleles by CRISPR/Cas mediated genome engineering. Cell *154*, 1370–1379.

Yao, X., Wang, X., Hu, X., Liu, Z., Liu, J., Zhou, H., Shen, X., Wei, Y., Huang, Z., Ying, W., et al. (2017). Homology-mediated end joining-based targeted integration using CRISPR/Cas9. Cell Res. *27*, 801–814.

Yoshimi, K., Kunihiro, Y., Kaneko, T., Nagahora, H., Voigt, B., and Mashimo, T. (2016). ssODN-mediated knock-in with CRISPR-Cas for large genomic regions in zygotes. Nat. Commun. *7*, 10431.

Yu, J., Vodyanik, M.A., Smuga-Otto, K., Antosiewicz-Bourget, J., Frane, J.L., Tian, S., Nie, J., Jonsdottir, G.A., Ruotti, V., Stewart, R., et al. (2007). Induced pluripotent stem cell lines derived from human somatic cells. Science *318*, 1917.

Yusa, K., Rashid, S.T., Strick-Marchand, H., Varela, I., Liu, P.-Q., Paschon, D.E., Miranda, E., Ordóñez, A., Hannan, N., Rouhani, F.J., et al. (2011). Targeted gene correction of α(1)-antitrypsin deficiency in induced pluripotent stem cells. Nature *478*, 391–394.

Zetsche, B., Gootenberg, J.S., Abudayyeh, O.O., Slaymaker, I.M., Makarova, K.S., Essletzbichler, P., Volz, S., Joung, J., van der Oost, J., Regev, A., et al. (2015). Cpf1 is a single RNA-guided endonuclease of a class 2 CRISPR-Cas system. Cell *163*, 759–771.

Zhang, J.-P., Li, X.-L., Li, G.-H., Chen, W., Arakaki, C., Botimer, G.D., Baylink, D., Zhang, L., Wen, W., Fu, Y.-W., et al. (2017). Efficient precise knockin with a double cut HDR donor after CRISPR/Cas9-mediated double-stranded DNA cleavage. Genome Biol. *18*, 35.

Zhang, J.-P., Li, X.-L., Neises, A., Chen, W., Hu, L.-P., Ji, G.-Z., Yu, J.-Y., Xu, J., Yuan, W.-P., Cheng, T., et al. (2016). Different effects of sgRNA length on CRISPR-mediated gene knockout efficiency. Sci. Rep. *6*, 28566.

Zhang, X.-B. (2013). Cellular reprogramming of human peripheral blood cells. Genomics Proteomics Bioinformatics *11*, 264–274.

Zou, J., Maeder, M.L., Mali, P., Pruett-Miller, S.M., Thibodeau-Beganny, S., Chou, B.-K., Chen, G., Ye, Z., Park, I.-H., Daley, G.Q., et al. (2009). Gene targeting of a disease-related gene in human induced pluripotent stem and embryonic stem cells. Cell Stem Cell *5*, 97–110.